

Expanding and Collapsing Scalar Field Thin Shell

M. Sharif *and G. Abbas †

Department of Mathematics, University of the Punjab,
Quaid-e-Azam Campus, Lahore-54590, Pakistan.

Abstract

This paper deals with the dynamics of scalar field thin shell in the Reissner-Nordström geometry. The Israel junction conditions between Reissner-Nordström spacetimes are derived, which lead to the equation of motion of scalar field shell and Klein-Gordon equation. These equations are solved numerically by taking scalar field model with the quadratic scalar potential. It is found that solution represents the expanding and collapsing scalar field shell. For the better understanding of this problem, we investigate the case of massless scalar field (by taking the scalar field potential zero). Also, we evaluate the scalar field potential when p is an explicit function of R . We conclude that both massless as well as massive scalar field shell can expand to infinity at constant rate or collapse to zero size forming a curvature singularity or bounce under suitable conditions.

Keywords: Gravitational collapse, Israel junction conditions; Scalar field.

PACS: 04.20.-q; 04.40.Dg; 97.10.CV

1 Introduction

The idea of the geon (electromagnetic-gravitational entity) by Wheeler *et al.* [1, 2] leads to investigation of scalar field in general relativity (GR). In GR,

*msharif.math@pu.edu.pk

†abbasg91@yahoo.com

the scalar field appears in the low energy limit of string theory [3]. Still, there is no observational evidence about the existence of such particles that are associated with the scalar field. However, the study of gravitational collapse of compact objects in the scalar-tensor theories imply that scalar field might be the source of scalar gravitational waves that can be detected by the advanced detectors [4]. Further, the observational facts from the binary pulsar may include or exclude the presence of scalar field in GR [5]. In astrophysical context, boson stars are such compact objects that are composed of scalar field. Probably, such stars were created in the early universe as Higgs particles condensate [6]. Recently, it has been proposed that boson stars are the candidates for dark matter [7]. Also, some remarkable similarities are suggested between neutron and boson stars.

Dynamics of scalar fields has been the subject of particular interest in both cosmological as well as astrophysical situations. In cosmological scenarios, scalar fields have a great attraction because such fields act as an effective cosmological constant in deriving the inflation. The nature of spacetime singularity for massless scalar field has been investigated in recent years on spherical collapse models [8]-[15]. Bhattacharya *et al.* [16] discussed the gravitational collapse of a minimally coupled massless scalar field and examined the possibility of existence of nonsingular models where collapse could be freezed under suitable conditions. All these studies investigate the dynamics of massless scalar field using the exact solutions of the field equations. Kaup [6] was among the pioneers to study complex massive scalar field configuration. Ruffini and Bonazzola [17] explored spherically symmetric system and determined the equilibrium conditions for boson stars solutions.

There is another formalism to study the dynamics of the matter field referred to as "*thin shell formalism*" developed by Israel [18]. This is one of the exactly solvable formulation in GR which is widely used to understand gravitational collapse and other cosmological as well as astrophysical processes. It involves a discontinuity of the extrinsic curvatures of the interior and exterior regions across a boundary surface. The jump in the extrinsic curvature across the boundary surface is caused by a thin layer of matter. In this formulation, the set of equations leads to equations of motion (much simpler) corresponding to the field equations, involving curvature on one side and matter on the other side. The solution of these equations provides full understanding of the dynamics of system. In the relativistic astrophysics, the thin shell equations help to study the properties of the compact objects.

Pereira and Wang [19] studied gravitational collapse of the cylindrical

shell made of counter rotating dust particles by using the Israel thin shell formalism. Sharif *et al.* [20]-[22] have investigated plane and spherically symmetric gravitational collapse by using this formulation. This approach was generalized to thin charged shell without pressure by De La Cruz and Israel [23]. Kuchar [24] and Chase [25] treated the charged thin shell problem with pressure by using polytropic equation of state. There are a number of papers devoted to handle the charged thin shell problems. Boulware [26] studied the time evolution of the charged thin shell and showed that their collapse could form a naked singularity if and only if density is negative. Farrugia and Hajicek [27] investigated third law of black hole mechanics in the Reissner Nordström (RN) geometry. Núñez [28] studied the oscillating perfect fluid shell. Also, Núñez *et al.* [29] explored the stability and dynamical behavior of the real scalar field for the Schwarzschild geometry in single null coordinate.

The purpose of the present paper is to study the application of Israel thin shell formalism for the scalar fields in the context of GR. In particular, we study the dynamical behavior of scalar field thin shell in charged background. To this end, we take interior and exterior regions as RN solutions, the Israel thin shell formalism is used to derive equations of motion of the shell for the perfect fluid. We then specify that the perfect fluid is generated by scalar field which leads to scalar field equations of motion. The solution of these equations provide expanding, collapsing or oscillating scalar field shell. The plan of the paper is as follows: Equations of motion for scalar field model with quadratic potential and their physical interpretation are presented in section 2. Sections 3 and 4 deal with dynamics of the massless and massive scalar field with arbitrary scalar potential, respectively. We summarize our results in the last section.

2 Dynamical Equations

In this section, we use Israel thin shell formulation to derive equations of motion of the scalar field shell. For this purpose, we take a $3D$ spacelike boundary surface Σ , which splits the two $4D$ spherically symmetric spacetimes V^+ and V^- . The interior and exterior regions V^- and V^+ , respectively are described by the RN metrics given by

$$(ds)_{\pm}^2 = \eta_{\pm} dT^2 - \frac{1}{\eta_{\pm}} dR^2 - R^2(d\theta^2 + \sin^2\theta d\phi^2), \quad (1)$$

where $\eta_{\pm}(R) = 1 - \frac{2M_{\pm}}{R} + \frac{Q_{\pm}^2}{R^2}$, M_{\pm} and Q_{\pm} are the mass and charge, respectively. The subscripts $+$ and $-$ represent quantities in exterior and interior regions to Σ , respectively. Further, it is assumed that charge in both regions is the same, i.e., $Q_- = Q_+ = Q$. The strength of the electric field on the shell can be described by the Maxwell field tensor, $F_{TR} = \frac{Q}{R^2} = -F^{RT}$.

The energy-momentum tensor of the electromagnetic field is

$$T_{\delta}^{\nu(em)} = \frac{1}{4\pi}(-F^{\nu\lambda}F_{\delta\lambda} + \frac{1}{4}\delta_{\delta}^{\nu}F_{\pi\lambda}F^{\pi\lambda}). \quad (2)$$

By employing the intrinsic coordinates (τ, θ, ϕ) on Σ at $R = R(\tau)$, the metrics (1) on Σ become

$$(ds)_{\pm\Sigma}^2 = [\eta(R) - \frac{1}{\eta(R)}(\frac{dR}{dT})^2]dT^2 - R^2(\tau)(d\theta^2 + \sin^2\theta d\phi^2). \quad (3)$$

Here T is also a function of τ and it is assumed that $g_{00} > 0$, so that T is a timelike coordinate. Also, the induced metric on the boundary surface Σ is given by

$$(ds)_{\Sigma}^2 = d\tau^2 - a^2(\tau)(d\theta^2 + \sin^2\theta d\phi^2). \quad (4)$$

The continuity of the first fundamental form gives

$$[\eta(R_{\Sigma}) - \frac{1}{\eta(R_{\Sigma})}(\frac{dR_{\Sigma}}{dT})^2]^{\frac{1}{2}}dT = (d\tau)_{\Sigma}, \quad R(\tau) = a(\tau)_{\Sigma}. \quad (5)$$

Now the unit normal n_{μ}^{\pm} to Σ in V^{\pm} coordinates can be evaluated as

$$n_{\mu}^{\pm} = (-\dot{R}(\tau), \dot{T}, 0, 0), \quad (6)$$

where dot represents differentiation with respect to τ .

The non-vanishing components of the extrinsic curvature are

$$K_{\tau\tau}^{\pm} = \frac{d}{dR}\sqrt{\dot{R}^2 + \eta_{\pm}}, \quad K_{\theta\theta}^{\pm} = -R\sqrt{\dot{R}^2 + \eta_{\pm}}, \quad K_{\phi\phi}^{\pm} = K_{\theta\theta}^{\pm}\sin^2\theta. \quad (7)$$

The surface energy-momentum tensor is defined by

$$S_{ij} = \frac{1}{\kappa}\{[K_{ij}] - \gamma_{ij}[K]\}, \quad (8)$$

where κ is a coupling constant, γ_{ij} is induced metric on Σ and

$$[K_{ij}] = K_{ij}^+ - K_{ij}^-, \quad [K] = \gamma^{ij}[K_{ij}]. \quad (9)$$

The surface energy-momentum tensor for a perfect fluid is

$$S_{ij} = (\rho + p)u_i u_j - p\gamma_{ij}, \quad (10)$$

where $u_i = \delta_i^0$. Using Eqs.(5), (8) and (10), we can find

$$\rho = \frac{2}{\kappa R^2}[K_{\theta\theta}], \quad p = \frac{1}{\kappa}\left\{K_{tt} - \frac{[K_{\theta\theta}]}{R^2}\right\}. \quad (11)$$

Inserting the non-zero components of the extrinsic curvature components, we get

$$(\zeta_+ - \zeta_-) + \frac{\kappa}{2}\rho R = 0, \quad (12)$$

$$\frac{d}{dR}(\zeta_+ - \zeta_-) + \frac{1}{R}(\zeta_+ - \zeta_-) - \kappa p = 0, \quad (13)$$

where $\zeta_{\pm} = \sqrt{\dot{R}^2 + \eta_{\pm}}$. Making use of Eq.(12) in (13), it follows that

$$\dot{m} + p\dot{A} = 0, \quad (14)$$

where $m(= \rho A)$ and $A(= 4\pi R^2(\tau))$ stand for the integrated total energy density at some time and area of the shell, respectively. The conservation of surface energy-momentum tensor leads to the same equation as Eq.(14) and hence this equation is known as energy conservation law on the shell. It is mentioned here that this equation can be solved by using the equation of state $p = k\rho$, and its solution is

$$\rho = \rho_0 \left(\frac{R_0}{R}\right)^{2(k+1)}, \quad (15)$$

where R_0 is the position of the shell at $t = t_0$ and ρ_0 is the density of matter on the shell at position R_0 . Using this value of ρ in the definition of m , we obtain

$$m = 4\pi\rho_0 \frac{R_0^{(2k+2)}}{R^{2k}}. \quad (16)$$

From Eq.(12), equation of motion of the shell is given by

$$\dot{R}^2 + V_{eff}(R) = 0, \quad (17)$$

where the effective potential $V_{eff}(R)$ is

$$V_{eff}(R) = 1 - \left(\frac{M_+ - M_-}{m}\right)^2 + \left(\frac{Q}{R}\right)^2 - \frac{(M_+ + M_-)}{R} - \left(\frac{m}{2R}\right)^2. \quad (18)$$

Notice that we have used $\kappa = 8\pi$ to derive this equation.

To see the effects of charge parameter Q on the dynamics of shell, we re-write Eq.(17) by using the above equation as follows

$$\dot{R} = \pm \sqrt{\left(\frac{M_+ - M_-}{m}\right)^2 - \left(\frac{Q}{R}\right)^2 + \frac{(M_+ + M_-)}{R} + \left(\frac{m}{2R}\right)^2} - 1. \quad (19)$$

Here $+$ ($-$) correspond to expansion (collapse) of shell and m is the same as defined after Eq.(14). The term $\frac{Q^2}{R^2}$ (Coulomb repulsive force) in \dot{R} (velocity of shell with respect to stationary observer) indicates that charge reduces velocity of the shell with respect to stationary observer. This velocity also depends on position of the observer, whether the observer is located inside or outside the shell. Further, Eq.(18) implies that charge parameter increases the effective potential V_{eff} . In coming sections, we shall see that throughout the dynamics of shell (composed of either massless or massive scalar field), charge parameter reduces and increases velocity of the shell with respect to stationary observer and V_{eff} , respectively. Thus initially the velocity of the shell with respect to stationary observer in the RN background is slower as compared to the Schwarzschild case (as shown in Figure 1). We conclude that electrostatic repulsive force in RN background tries to balance with the gravitational force due to the shell and hence the shell velocity with respect to stationary observer is slow in this case as compared to uncharged case.

In order to study the dynamics of scalar field shell, we specify that the perfect fluid is generated by a scalar field. The energy density and the pressure of the scalar field can be written as

$$\rho = \frac{1}{2}[\phi, \nu \phi, \nu + 2V(\phi)], \quad p = \frac{1}{2}[\phi, \nu \phi, \nu - 2V(\phi)], \quad (20)$$

where $V(\phi) = \tilde{m}^2 \phi^2$ is the potential term which contributes to provide mass of the scalar field. We note that the scalar field will be massless in the absence of such term. Using Eq.(20), we can write the energy-momentum tensor of the scalar field as follows

$$S_{ij} = \nabla_i \phi \nabla_j \phi - \gamma_{ij} \left[\frac{1}{2}(\nabla \phi)^2 - V(\phi) \right]. \quad (21)$$

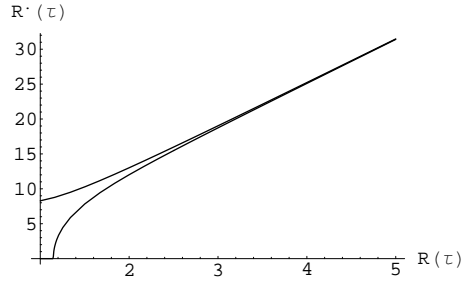


Figure 1: Behavior of the shell velocity with respect to stationary observer, when $M_+ = 1$, $M_- = 0$, $k = \rho_0 = R_0 = 1$ and $Q = 1$. The upper and lower curves correspond to uncharged and charged cases, respectively. It is clear that initially velocity in the charged case is less than the uncharged case. Velocities in both cases match for larger values R , as term $\frac{Q^2}{R^2}$ becomes negligible for larger values R

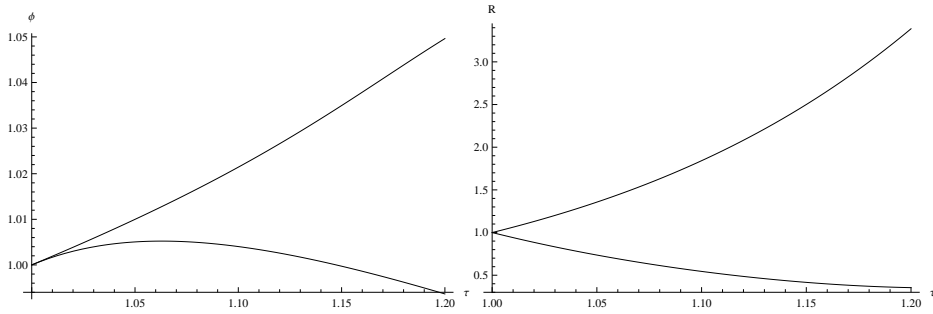


Figure 2: The left graph is the behavior of the shell radius R while the right graph is the behavior of scalar field. Both these graphs have been plotted by using $M_+ = 1$, $\tilde{m} = 1$, $M_- = 0$, $Q = 1$, $\dot{\phi}(1) = 0.19$ and $\phi(1) = R(1) = 1$.

Since the induced metric (4) depends only on τ , so ϕ also depends on τ . Thus Eq.(20) leads to

$$\rho = \frac{1}{2}[\dot{\phi}^2 + 2V(\phi)], \quad p = \frac{1}{2}[\dot{\phi}^2 - 2V(\phi)]. \quad (22)$$

In terms of the scalar field, the integrated total energy density of the shell at some time is

$$m = 2\pi R^2[\dot{\phi}^2 + 2V(\phi)]. \quad (23)$$

Using Eqs.(22) and (23) in Eq.(14), we get

$$\ddot{\phi} + \frac{2\dot{R}}{R}\dot{\phi} + \frac{\partial V}{\partial \phi} = 0. \quad (24)$$

This is the Klien-Gordon (KG) equation, $\square\phi + \frac{\partial V}{\partial \phi} = 0$, in coordinate system of the shell metric (4). In terms of the scalar field, the effective potential is

$$\begin{aligned} V_{eff}(R) &= 1 - \left(\frac{M_+ - M_-}{2\pi R^2(\dot{\phi}^2 + 2V(\phi))} \right)^2 + \left(\frac{Q}{R} \right)^2 - \frac{(M_+ + M_-)}{R} \\ &- [\pi R(\dot{\phi}^2 + 2V(\phi))]^2. \end{aligned} \quad (25)$$

Now we solve the KG equation (24) and equation of motion (17) (with Eq.(25)) simultaneously for $\phi(\tau)$ and $R(\tau)$. In this case, the exact solution is not possible. We solve these equations numerically by assuming the following initial conditions: $\dot{\phi}(1) = 0.19$ and $\phi(1) = R(1) = 1$. The graphs of these equations for the set of initial data are shown in Figure 2. The left graph shows the behavior of the shell radius R in which upper and lower curves represent the expanding and collapsing shell, respectively. The right graph is the behavior of scalar field whose upper and lower curves represent the collapsing and expanding shell, respectively. In case of collapse (upper curve), scalar field density ϕ goes on increasing while in case of expansion (lower curve), this comes to a point on τ -axis implying that scalar field decays to zero value in this case.

3 Massless Scalar Field

A scalar field becomes massless, when scalar potential, $V(\phi)$, is zero. In this case, the KG equation reduces to $\ddot{\phi} + \frac{2\dot{R}}{R}\dot{\phi} = 0$ whose solution is $\dot{\phi} = \frac{\Omega}{R^2}$,

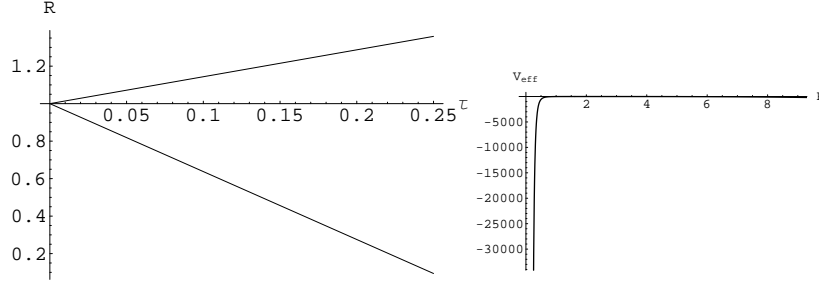


Figure 3: The left graph shows the shell radius for massless scalar field case (Eq.(26)). The right graph is the effective potential for massless scalar field (Eq.(28)) with $\Omega = 1$, keeping all the remaining parameters and initial conditions fixed as in Figures 1, 2.

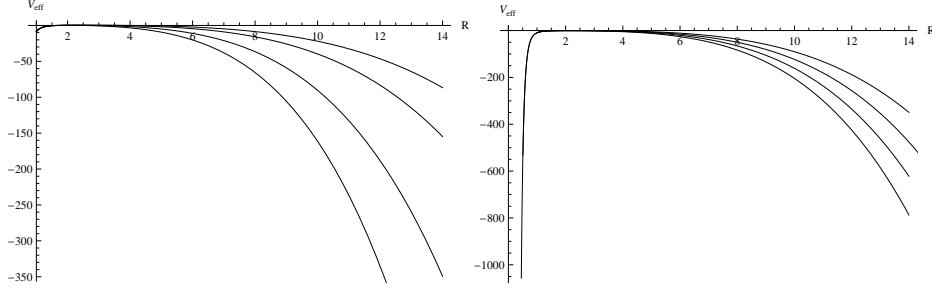


Figure 4: This figure describes the behavior of effective potential (Eq.(28)). Both graphs correspond to varying M_+ and M_- , keeping the remaining parameters fixed as in previous cases.

where Ω is an integration constant. Thus the equation of motion (17) with Eq.(25) takes the form

$$\dot{R}^2 + 1 - \left(\frac{M_+ - M_-}{2\pi\Omega^2} \right)^2 R^4 + \left(\frac{Q}{R} \right)^2 - \frac{(M_+ + M_-)}{R} - \frac{\pi^2\Omega^4}{R^6} = 0. \quad (26)$$

We define the following two parameters:

$$[M] = M_+ - M_-, \quad \overline{M} = \frac{M_+ + M_-}{2}.$$

Using these in Eq.(26), it follows that

$$\dot{R}^2 + V_{eff} = 0, \quad (27)$$

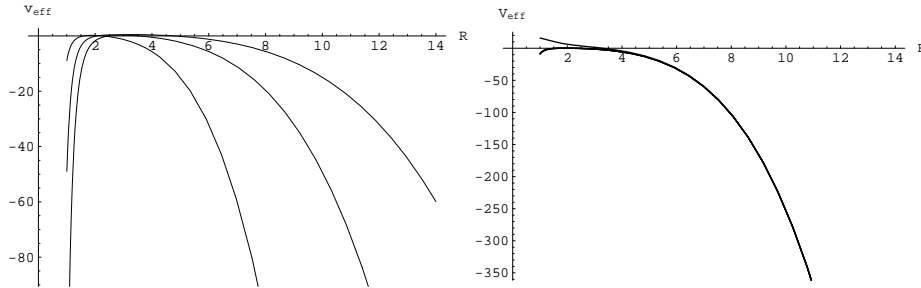


Figure 5: The left graph describes the effective potential for massless scalar field with different values of Ω , keeping all the remaining parameters fixed as in previous cases. The right graph represents the behavior of the massless scalar field shell for different values of the charge Q .

where

$$V_{eff} = 1 - \left(\frac{[M]}{2\pi\Omega^2} \right)^2 R^4 + \left(\frac{Q}{R} \right)^2 - \frac{2\bar{M}}{R} - \frac{\pi^2\Omega^4}{R^6}. \quad (28)$$

For the initial data of the shell, the left graph in Figure 3 shows the increase and decrease in shell radius implying the expansion and collapse of the massless scalar field shell. Thus a massless scalar shell may expand or collapse depending on the sign of velocity (i.e., \dot{R}) of the shell with respect to stationary observer. The behavior of the potential depends on the number of roots of the potential. If there is no root then the scalar field shell either expands indefinitely or collapses to a zero size from some finite value. If there is one non-degenerate root then the shell expands to infinity or contracts to some finite size. For one degenerate root, the shell will be in an unstable equilibrium or collapses to form a black hole or naked singularity [30].

The graphical representation of the effective potential with fixed parametric values of the model is shown in Figures 4, 5. Both graphs for varying M_+ and M_- in Figure 4 and the left graph in Figure 5 show that the effective potential diverges for initial values of R and then $V_{eff} \rightarrow -\infty$ as $R \rightarrow \infty$. In these cases, the shell expands to infinity or collapses to zero size. The right graph in Figure 5 shows that the effective potential has one root and there occurs unstable situation, after which potential diverges negatively and shell expands or collapses. The cases in which collapse occurs, the shell collapses to zero size by forming a curvature singularity at which intrinsic Ricci scalar of the shell, $R^\mu{}_\mu = -\frac{2}{R^2}(2R\ddot{R} + \dot{R}^2)$, diverges.

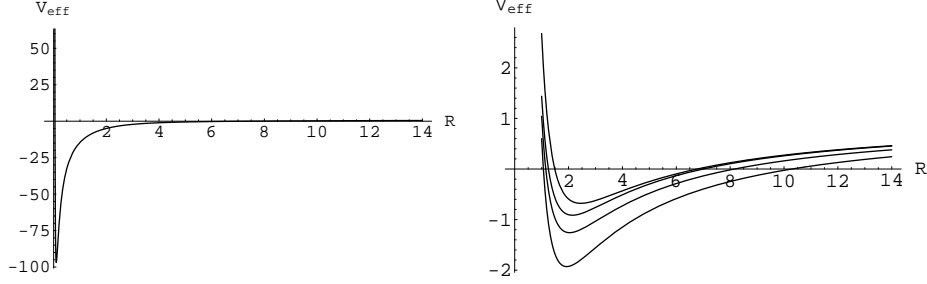


Figure 6: The behavior of effective potential for massive scalar field is shown for fixed parameters as well with varying charge parameter.

4 Massive Scalar Field

In this case, we discuss the motion of a scalar field for which potential term, $V(\phi)$ is determined by taking p as an explicit function of R . From Eq.(22), we get

$$\dot{\phi}^2 = p + \rho, \quad V(\phi) = \frac{1}{2}(p - \rho). \quad (29)$$

Also, from Eqs.(12) and (13), we get

$$\frac{d\rho}{dR} + \frac{2}{R}(p + \rho) = 0. \quad (30)$$

Here we use p as an explicit function of R , [29] i.e., $p = p_0 e^{-kR}$, where p_0 and k are constants. Inserting this value of p in Eq.(30), it follows that

$$\rho = \frac{\chi}{R^2} + \frac{2(1+kR)p_0 e^{-kR}}{k^2 R^2}, \quad (31)$$

where χ is constant of integration. Notice that the above equations satisfy the conservation equation (14). Further, applying the values of p and ρ in Eq.(29), we get

$$V(\phi) = \frac{\chi}{2R^2} - \frac{p_0 e^{-kR}}{2} \left(1 - \frac{2(1+kR)}{k^2 R^2} \right), \quad (32)$$

$$\dot{\phi}^2 = \frac{\chi}{R^2} + p_0 e^{-kR} \left(1 + \frac{2(1+kR)}{k^2 R^2} \right). \quad (33)$$

These equations satisfy the KG equation (24). Using Eqs.(29)-(32) in (25), we have

$$V_{eff}(R) = 1 - \left(\frac{M_+ - M_-}{m}\right)^2 + \left(\frac{Q}{R}\right)^2 - \frac{(M_+ + M_-)}{R} - \left(\frac{m}{2R}\right)^2, \quad (34)$$

where

$$m = 4\pi R^2 \rho \equiv 4\pi\chi + \frac{8\pi p_0 e^{-kR}}{k^2}(1 + kR). \quad (35)$$

The behavior of effective potential for massive scalar field shell is shown in Figure 6. The left graph is effective potential for massive scalar field (Eq.(34)) for $k = 1$, $\chi = 3$, $p_0 = 1$ and remaining parameters are fixed as in the massless scalar field case. This implies that $V_{eff} \rightarrow -\infty$ as $R \rightarrow 0$, the massive shell collapses to zero size forming a curvature singularity. The right graph represents effective potential for massive scalar field shell for different values of Q . There appear oscillations in the system. There exist such values of charge parameter for which scalar field shell executes an oscillatory motion. The oscillations occur at two points where V_{eff} cuts the horizontal axis at more than one point. The values of R for which $V_{eff} = 0$ are shown in right graph of Figure 6 yielding zero velocity. This implies that the shell stops for a moment and then expands or collapses. During the collapsing phase at minimum values of the radius, the tangential pressure reaches its maximum values while during the expansion, minimum pressure occurs at maximum radius. In this way, scalar field shell performs the oscillatory motion. The values of R for which $V_{eff} = 0$, and intrinsic curvature of the shell is finite, are bouncing points after bounce the shell either expands or collapse.

5 Discussion

In this paper, we have examined the dynamical behavior of the scalar field thin shell. Using the Israel formalism, the equations of motion have been formulated by taking the internal and external regions to the boundary surface as RN solution. The equations of motion are originally derived for perfect fluid and then are written in terms of scalar field. The complete dynamics of the thin shell is described by the equation of motion (17) and the KG equation (24). The exact solution of these equations cannot be found, however can be solved numerically. Firstly, we have solved these equations by using the scalar field potential as quadratic potential. This solution is shown in

Figures **1**, **2** which represents the collapsing and expanding scalar field shell. It has been found that scalar field decays out in the case of expansion while it grows in the case of collapse.

To analyze further, we have taken massless scalar field and a massive scalar field with p as an explicit function of R . In the case of massless scalar field, it has been found that the shell radius is an increasing or decreasing function of the proper time implying that the shell either collapses or expands. In this case, the effective potential (Figures **3-5**) predicts that shell can collapse to zero size by forming a curvature singularity or can expand to infinity. For the massive scalar field case with p as an explicit function of R , we have evaluated the scalar field potential instead of taking it as quadratic. It has been found that the shell radius behaves like the massless scalar field and the effective potential (Figure **6**) diverges negatively as the radius of the shell approaches to zero and oscillating behavior is noted in this case. This indicates that the shell collapses to zero size forming a curvature singularity. There is also bouncing behavior of the shell in this case. In the both (massless and massive scalar field) cases, when shell collapses, the edge of the shell coincides with the horizons of the interior black hole.

The results can be summarized as follows. We have found that there are three possible phases (expanding, collapsing and oscillating (bouncing)) during the dynamics of the scalar field in the present configuration. When shell expands, it continues expanding forever with constant velocity as the boundary surface is described by the spatially homogenous spacetime. In case of collapse, a shell collapses to zero size forming a curvature singularity at $R = 0$, where intrinsic Ricci scalar $R^\mu{}_\mu = -\frac{2}{R^2}(2R\dot{R} + \dot{R}^2)$, diverges. Also, the turning (bouncing) points occur when $V_{eff}(R) = 0$ at more than one value of R . In this case, the oscillations occur between two points where $V_{eff} = 0$. The values of R for which $V_{eff} = 0$ (right graph in Figure **6**), one gets zero velocity. This implies that the shell stops suddenly and then expands or collapses. During the collapse at $R = R_{min}$, the tangential pressure reaches to its maximal values while during expansion minimal pressure occurs $R = R_{max}$. In this way, the scalar field shell performs the oscillatory motion.

It would be interesting to extend this work for more generic geometry or using the polytropic equation of state to check the validity of cosmic censorship hypothesis.

Acknowledgment

We would like to thank the Higher Education Commission, Islamabad,

Pakistan for its financial support through the *Indigenous Ph.D. 5000 Fellowship Program Batch-IV*. Also, we highly appreciate the fruitful comments of the anonymous referees.

References

- [1] Wheeler, J.A.: Phys. Rev. **97**(1955)511.
- [2] Brill, D.R. and Wheeler, J.A.: Phys. Rev. **105**(1957)1662.
- [3] Damour, T. and Polyakov, A.M.: Gen. Relativ. Gravit. **26**(1994)1171.
- [4] Harada, T., Chiba, T., Nakao, K. and Nakamura, K.: Phys. Rev. **D55**(1997)2029.
- [5] Damour, T. and Esposito-Farese, C.: Phys. Rev. **D54**(1996)1476.
- [6] Kaup, D.J.: Phys. Rev. **172**(1968)1331.
- [7] Jetzer, P.: Phys. Rep. **220**(1992)163.
- [8] Christodoulou, D.: Ann. Math. **140**(1994)607.
- [9] Choptuik, M.W.: Phys. Rev. Lett. **70**(1993)9.
- [10] Evans, C.R. and Coleman, J.S.: Phys. Rev. Lett. **72**(1994)1782.
- [11] Roberts, M.D.: Gen. Relativ. Gravit. **21**(1989)907.
- [12] Bardy, P.R.: Class. Quantum Grav. **11**(1996)1255.
- [13] Malec, E.: Class. Quantum Grav. **13**(1995)1849.
- [14] Gundlach, C.: Phys. Rev. Lett. **75**(1995)3214.
- [15] Giambo, R., Giannon, F. and Magli, G.: J. Math. Phys. **49**(2008)042504.
- [16] Bhattacharya, S., Goswami, R. and Joshi, P.S: arXiv:0807.1985.
- [17] Ruffini, R. and Bonazzola, S.: Phys. Rev. **187**(1969)1767.
- [18] Israel, W.: Nuovo Cimento **B44**(1966)1; *ibid.* **B48**(1967)463(E).

- [19] Pereira, P.R.C.T. and Wang, A.: Phys. Rev. **D62**(2000)124001; Erratum *ibid.* **D67**(2003)129902.
- [20] Sharif, M. and Ahmad, Z.: Int. J. Mod. Phys. **A23**(2008)181.
- [21] Sharif, M. and Iqbal, K.: Mod. Phys. Lett. **A24**(2009)1533.
- [22] Sharif, M. and Abbas, G.: Gen. Relativ. Gravit. **43**(2011)1179.
- [23] De La Cruz, V. and Israel, W.: Nuovo Cimento **A51**(1967)744.
- [24] Kuchar, K.: Czechoslovak J. Phys. Section **B18**(1968)435.
- [25] Chase, J.E. : Nuovo Cimento **B67**(1970)136.
- [26] Boulware, D.G.: Phys. Rev. **D8**(1973)2363.
- [27] Farrugia, Ch.J. and Hajicek, P.: Commun. Math. Phys. **68**(1979)291.
- [28] Núñez, D.: Astrophys. J. **482**(1997)963.
- [29] Núñez, D., Quevedo, H. and Salgado, M.: Phys. Rev. **D58**(1998)083506.
- [30] Mann, R.B. and Oh, J.J.: Phys. Rev. **D74**(2006)124016.